# Dual function of C/D box small nucleolar RNAs in rRNA modification and alternative pre-mRNA splicing

Marina Falaleeva[a], Amadis Pages[b], Zaneta Matuszek[a], Sana Hidmi[c], Lily Agranat-Tamir[c], Konstantin Korotkov[a], Yuval Nevo[d], Eduardo Eyras[b,e], Ruth Sperling[c], and Stefan Stamm[a,1]

[a]Department of Molecular and Cellular Biochemistry, University of Kentucky, Lexington, KY 40536; [b]Department of Experimental and Health Sciences, Universitat Pompeu Fabra, E08003 Barcelona, Spain; [c]Department of Genetics, Hebrew University of Jerusalem, 91904 Jerusalem, Israel; [d]Department of Microbiology and Molecular Genetics, Computation Center at the Hebrew University and Hadassah Medical Center, 91904 Jerusalem, Israel; and [e]Catalan Institution for Research and Advanced Studies, E08010 Barcelona, Spain

Edited by James E. Dahlberg, University of Wisconsin Medical School, Madison, WI, and approved February 5, 2016 (received for review October 1, 2015)

**C/D box small nucleolar RNAs (SNORDs) are small noncoding RNAs, and their best-understood function is to target the methyltransferase fibrillarin to rRNA (for example, *SNORD27* performs 2′-*O*-methylation of A27 in 18S rRNA). Unexpectedly, we found a subset of SNORDs, including *SNORD27*, in soluble nuclear extract made under native conditions, where fibrillarin was not detected, indicating that a fraction of the *SNORD27* RNA likely forms a protein complex different from canonical snoRNAs found in the insoluble nuclear fraction. As part of this previously unidentified complex, *SNORD27* regulates the alternative splicing of the transcription factor *E2F7* pre-mRNA through direct RNA–RNA interaction without methylating the RNA, likely by competing with *U1* small nuclear ribonucleoprotein (snRNP). Furthermore, knockdown of *SNORD27* activates previously "silent" exons in several other genes through base complementarity across the entire *SNORD27* sequence, not just the antisense boxes. Thus, some SNORDs likely function in both rRNA and pre-mRNA processing, which increases the repertoire of splicing regulators and links both processes.**

alternative splicing | gene regulation | snoRNAs | pre-mRNA processing

Small nucleolar RNAs (snoRNAs) are 60- to 300-nt-long noncoding RNAs that accumulate in the nucleolus. Based on conserved sequence elements, snoRNAs are classified as C/D box small nucleolar RNAs (SNORDs) or H/ACA box snoRNAs (SNORAs). SNORDs contain sequence elements termed C (RUGAUGA) and D (CUGA) boxes, usually present in duplicates (C′ and D′ boxes), and up to two antisense boxes that hybridize to the target RNA (1). In humans, SNORDs are usually derived from introns. After the splicing reaction, introns are excised as lariats, which are then opened by the debranching enzyme and subsequently degraded. Intronic SNORDs escape this degradation by forming a protein complex that consists of non-histone chromosome protein 2-like 1 (NHP2L1, 15.5K, SNU13), nucleolar protein 5A (NOP56), nucleolar protein 5 (NOP58), and fibrillarin (2–4). The SNORD protein complex forms through the entry of the snoRNA and fibrillarin to a complex containing NHP2L1, NOP58, and at least five assembly factors (5). The SNORD acts as a scaffold for the final protein complex formation and also controls recognition of other RNAs using the antisense boxes. The antisense boxes recognize sequences in rRNA, resulting in the fifth nucleotide upstream of the D or D′ box being 2′-*O*-methylated by fibrillarin (1). Structural studies indicate that the active form of SNORDs is dimeric (6).

The conserved overall structure of SNORDs allows the identification of their putative target RNA binding sites. However, numerous SNORDs without obvious target RNAs have been identified (7–10) and are termed "orphan snoRNAs." Genome-wide deep sequencing experiments identified shorter but stable SNORD fragments that were found in all species tested, ranging from mammals to the protozoan *Giardia lamblia* (11) and Epstein–Barr virus (12). Fragments longer than 27 nt generated by SNORDs will likely not bind argonaute proteins that bind to 21- to 22-nt-long microRNAs. These differences in size indicate that most SNORD fragments are not microRNAs, which have an average length of 21–22 nt (13–16), and suggests that these fragments may have additional functions.

The association of some SNORDs with specific diseases suggests that they may possess functions in addition to directing the 2′-*O*-methylation of rRNA. For example, the loss of *SNORD116* expression is a decisive factor in Prader–Willi syndrome, the most common genetic cause for hyperphagia and obesity (17, 18). *SNORD60* is involved in intracellular cholesterol trafficking, which is independent of its suggested function in rRNA methylation (19), and SNORDs *U32a*, *U33*, and *U35a* mediate lipotoxic stress, possibly through their cytosolic function (20). Although SNORDs are considered housekeeping genes, the expression of some *SNORD*s is altered in cancer. For example, changes in the expression of *SNORD27*, *-30*, *-25*, and *-31* mark the progression of smoldering multiple myeloma (21), and *SNORD50* deletions are associated with prostate and breast cancer (22–24). Genome-wide comparison of SNORD expression between cancer and normal cells showed the presence of two classes of SNORDs that differ in their terminal stems but are made from the same SNORD hosting intron (25).

Studies in yeast have shown that cellular nutritional status can control the formation of SNORDs. A complex of four proteins [Rvb1, Rvb2, Tah1, and Phi1 (R2TP)] stabilizes NOP58 under conditions of growth. Under starving conditions, the R2TP complex localizes to the cytosol, destabilizing NOP58 formation and inhibiting small nucleolar ribonucleoprotein (snoRNP) formation (26, 27), suggesting that there is a cell program that regulates snoRNP composition.

## Significance

**C/D box small nucleolar RNAs (SNORDs) are abundant, short, nucleoli-residing, noncoding RNAs that guide the methyltransferase fibrillarin to perform 2′-*O*-methylation of target RNAs. We identified 29 SNORDs present in a fibrillarin-containing fraction as well as a fibrillarin-free fraction enriched in spliceosomes. One of these SNORDs, *SNORD27*, directs *rRNA* methylation and regulates alternative pre-mRNA splicing (AS) of *E2F7* pre-mRNA, a transcriptional repressor of cell cycle-regulated genes. *SNORD27* likely regulates *E2F7* pre-mRNA AS by masking splice sites through base pairing. This previously unidentified function of SNORDs increases the number of factors regulating AS, a critical step in the expression of the vast majority of human genes, and highlights a potential coupling between AS, cell cycle, proliferation, and ribosome biogenesis.**

Author contributions: M.F., E.E., R.S., and S.S. designed research; M.F., A.P., Z.M., S.H., L.A.-T., Y.N., and E.E. performed research; K.K. contributed new reagents/analytic tools; M.F., R.S., and S.S. analyzed data; and M.F., R.S., and S.S. wrote the paper.

The authors declare no conflict of interest.

This article is a PNAS Direct Submission.

[1]To whom correspondence should be addressed. Email: stefan@stamms-lab.net.

This article contains supporting information online at www.pnas.org/lookup/suppl/doi:10.1073/pnas.1519292113/-/DCSupplemental.

Taken together, these findings suggest that cells modify SNORDs expression, that SNORDs are structurally more diverse than previously recognized, and that SNORDs have additional cellular functions other than 2′-*O*-methylation of rRNAs.

A previously described noncanonical function of SNORDs is their influence on alternative exon selection. Alternative pre-mRNA splicing is a mechanism that controls the inclusion of exons and the retention of introns in mature mRNA. More than 94% of human genes are estimated to undergo alternative splicing (28, 29), which greatly increases the complexity of the transcriptome (30). For example, the neuron-specific *SNORD115* promotes the inclusion of an alternative exon in the *serotonin receptor 2C* pre-mRNA (31), and *SNORD88C* regulates alternative splicing of *FGFR3* pre-mRNA (32). Although proof of principle experiments have shown that methylation of the branch point adenosine by engineered snoRNAs can change alternative splicing (33–35), the mechanism by which SNORDs regulate splice site selection in vivo is not clear.

Here, we used a native isolation procedure to characterize SNORDs from the nucleoplasma (36, 37) that were soluble under physiological salt extraction conditions. These SNORDs were found in complexes with splicing factors, where fibrillarin was not detected. We characterized the cancer-relevant *SNORD27* in detail and found that it regulates alternative splicing of the *E2F7* transcription

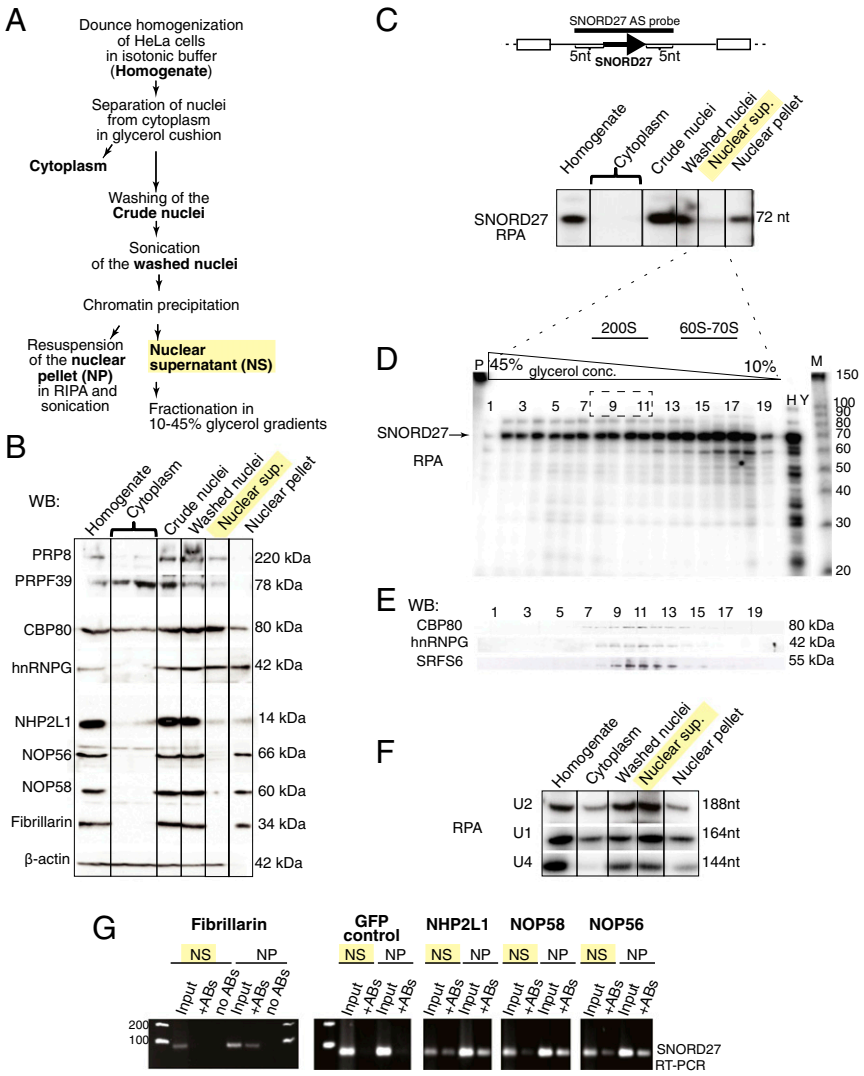


**Fig. 1.** A portion of *SNORD27* is present in a soluble nuclear fraction where fibrillarin is not detected. (*A*) The schematic representation of *HeLa* cell fractionation under native conditions. (*B*) Western blot analysis of the fractionation described in *A*; 5% of the total volume of each fraction prepared was analyzed by Western blot. The components of spliceosomes (PRP8 and PRPF39), splicing regulators (CBP80/NCBP1 and hnRNPG), and constitutive SNORD binding proteins (NHP2L1/15.5K, NOP56, NOP58, and fibrillarin) were detected by specific antibodies. (*C*) Distribution of *SNORD27* in cellular fractions determined by RPA. The diagram shows the *SNORD27* expression cassette and the location of the RPA probe. The arrow indicates *SNORD27*, and boxes indicate hosting exons. The RPA probe spanned the annotated *SNORD27* sequence and 5 nt from the surrounding intron. (*D*) Separation of the soluble nuclear supernatant fraction in a glycerol gradient. Nuclear supernatant (*C*) was separated on 10–45% glycerol gradient. The gradient was subdivided into 20 fractions; RNA from 50% of each fraction was isolated and analyzed by RPA with an *SNORD27* antisense probe. The arrow shows full-length *SNORD27*. (*E*) Individual glycerol gradient fractions were analyzed by Western blotting using antibodies recognizing markers for pre-mRNA processing: CBP80, hnRNPG, and SRSF6. (*F*) The distribution of *U1, U2*, and *U4* snRNAs in the fractions obtained by *HeLa* cell fractionation (*A*) was determined by RPA. (*G*) Association of *SNORD27* with constitutive SNORD binding proteins. Endogenous fibrillarin and Flag-tagged NHP2L1, NOP58, and NOP56 were immunoprecipitated and copurified. *SNORD27* was then detected by RT-PCR. Cells transfected with GFP were used as a control. +Abs, immunoprecipitated with the depicted antibodies; H, 10 μg total *HeLa* RNA; M, molecular weight size marker; NP, nuclear pellet; NS, nuclear supernatant; P, untreated probe; WB, Western blot; Y, 10 μg total yeast RNA.

factor pre-mRNA through direct RNA interaction and suppresses silent exon inclusion in *MAP4K3*, *ZBTB37*, *FER*, and *ABCA8* pre-mRNAs. These silent exons are not expressed in the presence of *SNORD27* and were previously not described. The data show that SNORDs are structurally diverse and have, in addition to their role in rRNA modification, an unexpected widespread function in pre-mRNA processing.

## Results

**Subset of SNORDs Is Present in a Nucleoplasmic Fraction Devoid of Fibrillarin.** To determine the possible function of SNORDs outside the nucleolus, we prepared a soluble nuclear extract using native salt conditions (*Materials and Methods* and Fig. 1*A*) (36, 37). In contrast to the method by Dignam et al. (38) that uses 420 mM KCl and 1 mM DTT for extraction, this method preserves higher-order splicing complexes, as previously determined by EM (36, 37). Western blot analysis showed that native nuclear supernatant contained splicing factors PRP8 and PRPF39 and pre-mRNA–associated proteins CBP80 and heterogeneous ribonucleoprotein G (hnRNPG) as expected (Fig. 1*B*). SNORDs associate with fibrillarin, NOP56, NOP58, and NHP2L1 to form a canonical snoRNP (3). In this complex, the methyltransferase fibrillarin catalyzes 2′-*O*-methylation of the targeted ribose residue (6). We noted that the nuclear supernatant contained small amounts of the SNORD-associated proteins NHP2L1, NOP56, and NOP58. Fibrillarin, however, was not detectable (Fig. 1*B*). All four constitutive components of SNORD-RNPs were present in the resuspended nuclear pellet (Fig. 1*B*).

The native nuclear supernatant was further fractionated using 10–45% (vol/vol) glycerol gradients (Fig. 1 *C*–*E*), and RNAs smaller than 200 nt from combined fractions 8–11 were analyzed by RNA sequencing (RNA-seq) (Fig. S1). In previous experiments, fractions corresponding to the analogous positions in the gradient were enriched for the five spliceosomal *U* snRNAs (37, 39–41) (Fig. S1*D*), various pre-mRNAs (36, 42, 43), and regulatory splicing factors (41, 44, 45) (Fig. 1*E*) and contained active spliceosomes (37).

Strikingly, in the fractions where fibrillarin was not detectable, we found a large number of full-length and shortened SNORDs, indicating that a large number of SNORDs exists in forms different from canonical fibrillarin-containing snoRNPs (Table S1).

For additional analysis, only the well characterized SNORDs annotated in the sno-LBME database (46) were considered. Using a threshold of 20 reads, we found 29 SNORDs in the spliceosomal fraction; 93 SNORDs were absent from the spliceosomal fraction but were expressed in *HeLa* cells as observed from the ENCODE sequencing data (47), and 137 SNORDs were not expressed in *HeLa* cells and subsequently, were not detected in the *HeLa* spliceosomal fraction. Thus, ∼24% of the SNORDs expressed in *HeLa* cells were found in spliceosomal fractions. In contrast, we found only five H/ACA snoRNAs and one small Cajal body-specific RNA (scaRNA) that showed 20 or more reads in the spliceosomal fractions, which represent less than 5% of the total number of known H/ACA snoRNAs and scaRNAs. Therefore, the majority of snoRNA reads were mapped to SNORDs and not mapped to other snoRNAs. Although we found a weak correlation between general SNORDs abundance and presence in the spliceosomal fractions (Spearman's rank correlation coefficient $r_s = 0.3$; $P < 0.0056$), a number of snoRNAs was clearly enriched in the spliceosomal fractions (Fig. S1*B* and Table S1). We detected the same proportion of orphan snoRNAs to total snoRNAs in both spliceosomal fractions and total *HeLa* RNA. In both cases, orphan snoRNAs comprised ∼11% of the total RNAs (when counting one snoRNA per cluster). Thus, close to one-quarter of expressed SNORDs are found in a fibrillarin-free fraction, without enrichment of orphan SNORDs.

We next determined the presence of *SNORD27* in different cellular fractions using an RNase protection assay (RPA), because this SNORD is deregulated in smoldering multiple myeloma (21). However, although *SNORD27* was mostly present in the resuspended nuclear pellet, it was also detectable in the native nuclear

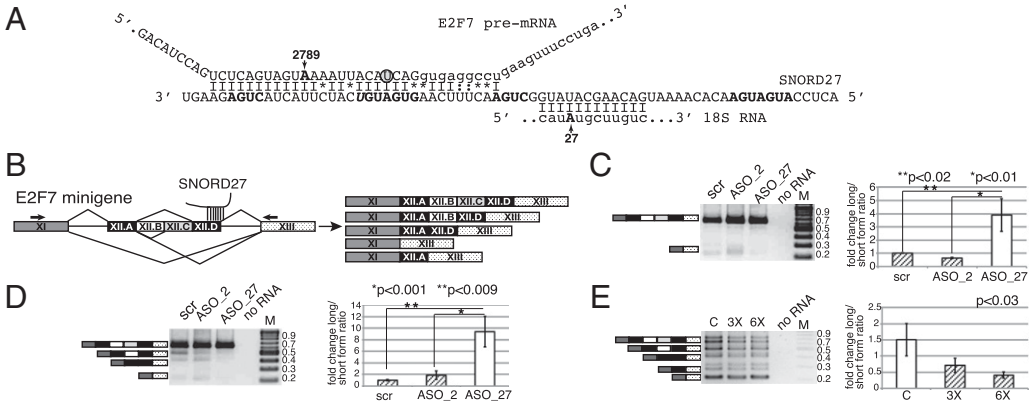


**Fig. 2.** *SNORD27* influences splicing of the E2F7 pre-mRNA. (*A*) Sequence alignment between *SNORD27*, *E2F7*, and *18S* rRNA. *SNORD27* is shown in the 3′→5′ direction; all other RNAs are shown in the 5′→3′ direction. The C and D boxes are indicated in bold. The nonconsensus U in the C′ box is indicated in bold italic. The adenosine residue A27 of the *18S* rRNA that undergoes 2′-*O*-methylation is indicated in bold. The putative 2′-*O*-methylation site on E2F7's A2789 (RefSeq NM_2033942) is indicated. Capital letters indicate the *E2F7* exon, and lowercase letters indicate the intron. The SNP rs310831 [CAT > CAA (H > Q)] in *E2F7* is indicated by a circle. (*B*) Gene structure and splicing pattern of the *E2F7* gene region regulated by *SNORD27*. The location of the *SNORD27* binding site is schematically indicated. Angled lines indicate splicing patterns. The splice products are shown in *Right*. (*C*) Effect of *SNORD27* knockdown on endogenous *E2F7* splicing. *HeLa* cells were transfected with *SNORD27* (ASO_27) or *SNORD2* (ASO_2) antisense or random base oligonucleotides. The location of the antisense oligonucleotides and the knockdown efficiency of the snoRNAs are shown in Fig. S4. The RNA was analyzed by RT-PCR using primers indicated in *B*. Graphs show the quantification of the splicing products. The ratio of the exon inclusion to exon skipping of untreated cells was set to one. The fold change is shown. Error bars are SDs of at least four independent experiments. The *P* value was determined using a two-tailed *t* test. (*D*) Analysis of *SNORD27* knockdown on *E2F7* minigene splicing. The gene region shown in *B* was cloned under a CMV promoter. *HeLa* cells were cotransfected with *E2F7* minigene and *SNORD27* (ASO_27) or *SNORD2* (ASO_2) antisense or random base oligonucleotides. The RNA was analyzed similar to in *C*. (*E*) Effect of *SNORD27* overexpression on *E2F7* splicing. An increasing amount of *SNORD27* expression construct was cotransfected with the *E2F7* minigene in porcine cells (*Porcine Aortic Endothelial*). C indicates no SNORD27 construct transfected, and 3× and 6× indicate threefold or sixfold molar ratio of SNORD27 construct to E2F7 minigene, respectively. The RNA was analyzed similar to in *C*. The *P* value was determined using one-way ANOVA test. M, molecular weight size marker; scr, random base oligonucleotide.

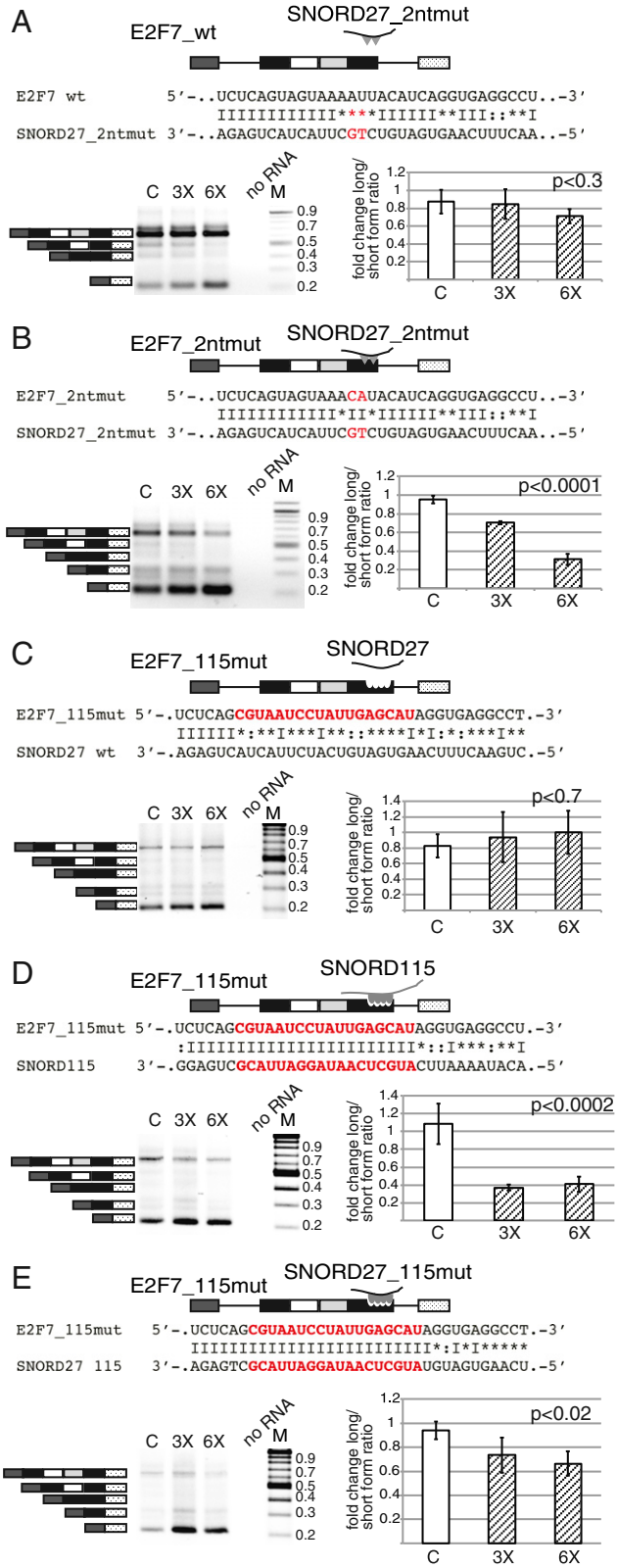


**Fig. 3.** Mutational analysis of *SNORD27–E2F7* interaction. The gels show RT-PCR analysis of *HeLa* cells cotransfected with SNORD27 WT or mutant construct and E2F7 WT or mutant minigene. The diagrams schematically show constructs that were used for cotransfection. The sequence alignment shows complementarity between cotransfected pairs, where the mutated sequences are shown in red. C indicates no SNORD27 construct transfected, and 3× and 6× indicate threefold or sixfold molar ratio of SNORD27 construct to E2F7 minigene, respectively. The ratio of the exon inclusion to exon skipping of untreated cells was set to one. The fold change is shown. Error bars are SDs of at least four independent experiments. The *P* values were determined using one-way ANOVA test. (*A*) WT E2F7 minigene was cotransfected with SNORD27_2nt mutant (binding site was changed by mutating two nucleotides in the complementary region that generated a 4-nt mismatch). (*B*) The E2F7 minigene was mutated (*E2F7_2ntmut*) to compensate for the changes in the *SNORD27_2nt* mutant. (*C*) The pre-mRNA serotonin receptor 2C sequences were introduced into the E2F7 minigene (E2F7_115mut) and cotransfected with WT *SNORD27*. (*D*) The E2F7_115mut minigene was cotransfected with the SNORD115 construct. (*E*) The E2F7_115mut minigene was cotransfected with an *SNORD27* construct containing the SNORD115 (MBII-52) binding site (SNORD27_115). M, molecular weight size marker.

supernatant (Fig. 1*C*). Next, nuclear supernatants were further fractionated using 10–45% glycerol gradients. The expected protected fragment of *SNORD27* is 72 nt long and present in all fractions (Fig. 1*D*). In addition, multiple shorter fragments were present in the gradients, with apparent lengths of 22, 30, and 50 nt that reflected some of the fragments observed in the RNA-seq experiments. Some of these RNAs are present in fractions 8–11 that contain most of the in vivo spliceosomes (37, 48) as determined by the presence of five spliceosomal *U* small nuclear ribonucleoproteins (snRNPs) (Fig. S1*D*) and regulatory splicing factors (Fig. 1*E*). As a control, we performed RPA using total *HeLa* RNA as well as yeast tRNA. The total *HeLa* RNA was isolated using TRIzol extraction, which solubilizes all RNAs, including those associated with nucleoli. In this preparation, the full-length *SNORD27* as well as multiple shorter fragments were detected (Fig. 1*D*). The presence of the spliceosomal components *U1*, *U2*, and *U4* snRNAs in the soluble nuclear fractions was confirmed by RPA (Fig. 1*F*), suggesting that a subset of SNORDs cosediments with spliceosomes.

To test whether other SNORDs determined by RNA-seq (Table S1) were present in a fibrillarin-free fraction, we analyzed the sedimentation of *SNORD2*, *SNORD60*, and *SNORD78* following the previously established characterization of spliceosome-containing fractions (37), (Fig. S1). The gradient was subdivided into four parts: A–D. Fraction A contained proteins that sedimented faster than 200S and was devoid of spliceosomes; fraction B contained supraspliceosomes that sedimented in the 200S region (37, 48, 49), fraction C contained native spliceosomes that sedimented at 60–70S (37, 41, 50), and fraction D contained proteins and small RNAs that appeared as free proteins or assembled into small RNP complexes. *SNORD2*, *SNORD60*, and *SNORD78* were present in fractions B and C associated with spliceosomes but devoid of fibrillarin (Figs. S2 and S3). This distribution suggests that numerous SNORDs exist in the cell without being associated with fibrillarin, but possibly, they may be associated with spliceosomes.

We next tested the association of *SNORD27* with SNORD-associated proteins directly. We performed immunoprecipitations using native nuclear supernatant and resuspended nuclear pellet using antibodies against Flag-tagged NHP2L1, NOP58, and NOP56 as well as endogenous fibrillarin. The immunoprecipitates were analyzed by RT-PCR using primers against *SNORD27* (Fig. 1*G*). As shown in Fig. 1*G*, *SNORD27* is readily detectable in all immunoprecipitates made from resuspended nuclear pellet. Confirming our previous results, we could not detect *SNORD27* in fibrillarin immunoprecipitates from soluble nuclear extract, which is consistent with the lack of fibrillarin detection in nuclear supernatant based on Western blot results (Fig. 1*B*). Trace amounts of *SNORD27* are detectable with NOP58 and NOP56, and a larger amount immunoprecipitates with NHP2L1.

We next analyzed the location of fibrillarin, NHP2L1, NOP58, and NOP56 in native soluble nuclear extract separated on glycerol gradients. Reflecting the immunoprecipitations, fibrillarin and NOP58 are absent from individual gradient fractions. NHP2L1 and NOP56 are concentrated in the lower-density part at the top of

the gradient but absent in higher-density parts (Fig. S3*A*), suggesting that *SNORD27* forms diverse protein–RNA complexes. In contrast, hnRNPG, heterogeneous ribonucleoprotein C1/C2 (hnRNPC1/C2), and ALY/REF as well as splicing factors SF3B1 and PRP8 and the nuclear cap binding protein CBP80 are present in all fractions, with hnRNPG and hnRNPC1/C2 present predominantly in fractions B and C (Fig. S3*B*).

Taken together, these data suggest that *SNORD27* is present in two biochemically separable fractions. In the insoluble nuclear fractions, it is associated with fibrillarin, NOP56, NOP58, and NHP2L1 and likely forms a canonical snoRNP. In the native soluble nuclear fraction, however, *SNORD27* is free from fibrillarin, and a part of *SNORD27* associates with NOP56 and NHP2L1, suggesting that *SNORD27* could have a function outside the canonical snoRNP.

**SNORD27 Regulates Alternative Splicing of E2F7 Pre-mRNA.** The presence of *SNORD27* in nuclear fractions devoid of fibrillarin suggests that it has a function apart from rRNA 2′-*O*-methylation. We previously found that the orphan *SNORD115* changes alternative splicing of the *serotonin receptor 2C* and several other pre-mRNAs, possibly through base pairing of *SNORD115* to a splicing regulatory region (31, 51). We, therefore, looked for complementarities between *SNORD27* and pre-mRNAs across the genome.

Because very little is currently known about the binding between SNORDs and their noncanonical targets, we performed a genome-wide search for potential targets using complementarities to the entire sequence of *SNORD27* and not just the antisense box involved in recognizing rRNA. We searched for targets of any length with at least 22 matching nucleotides and up to two mismatches and allowed any number of noncanonical (U:G) pairings (Table S2), concentrating on complementarities in the vicinity of alternative exons. One of the best complementarities was found between *SNORD27* and an alternatively spliced exon of the *E2F7* gene. The complementarity consisted of 29 nucleotides with two G:U pairs, four mismatched bases, and no gaps. Importantly, the sequence complementarity extended to five nucleotides of the alternative 5′ splice site (Fig. 2*A*). The alternative exon is longer (425 nt) than the average human cassette exon (147 nt) (52) and contains several internal splice sites (Fig. 2*B* and Table S3*A*). To test the functionality of the sequence complementarity to *SNORD27*, we knocked down *SNORD27* using modified chimeric antisense oligonucleotides. This approach was previously developed to knock down noncoding RNAs (ncRNAs), including intronic SNORDs, in *HeLa* cells (53). The oligonucleotides contained 10 phosphothioate DNA nucleotides surrounded by 5 2′-*O*-methyl–modified phosphorothioate RNA nucleotides at both the 5′ and 3′ ends. The oligonucleotides were designed to bind the antisense box of *SNORD27* and *SNORD2* located between C and D′ boxes (Fig. S4). The oligonucleotides reduced the amount of *SNORD27* by 80% (Fig. S4*B*). Oligonucleotides knocking down *SNORD2* by 95% were used as a negative control (Fig. S4*C*). The knockdown of *SNORD27* reduced alternative exon skipping fourfold (Fig. 2*C*). To allow for mechanistic studies, a minigene containing the alternative exon and its two flanking constitutive exons was constructed (Fig. 2*B*). Transfecting this construct into *HeLa* cells showed a similar pattern to the endogenous splicing event. However, use of an internal splice site in the exon was more prevalent in the minigene. Similar to the endogenous gene, an *SNORD27* knockdown reduced alternative exon skipping (Fig. 2*D*).

*SNORD27* depletion thus leads to an almost constitutive use of the alternative exon harboring the predicted binding site. Cotransfection of *E2F7* and *SNORD27* expression constructs did not increase *E2F7* alternative exon skipping in *HeLa* cells, likely because of the high level of endogenous expression of *SNORD27*. However, the *E2F7* sequence complementarity of *SNORD27* is only poorly conserved between pig and human (Table S3*B*); therefore, we cotransfected porcine (*Porcine Aortic Endothelial*) cells with human *E2F7* and human *SNORD27* expression constructs to avoid interference with endogenous *SNORD27*. We observed an *SNORD27* concentration-dependent increase in the *E2F7* exon skipping. At the highest ratio, the alternative exon was predominantly skipped, further confirming that *SNORD27* blocks use of the alternative splice site (Fig. 2*E*).

In summary, these data show that *SNORD27* blocks use of an alternative exon in *E2F7* pre-mRNA.

**Sequence Complementarity Between SNORD27 and E2F7 Is Necessary for Splicing Regulation.** To determine whether a direct *SNORD27*–*E2F7* RNA interaction is necessary for regulation, we used a compensatory mutation approach. We mutated two nucleotides in the region of sequence complementarity between *SNORD27* and

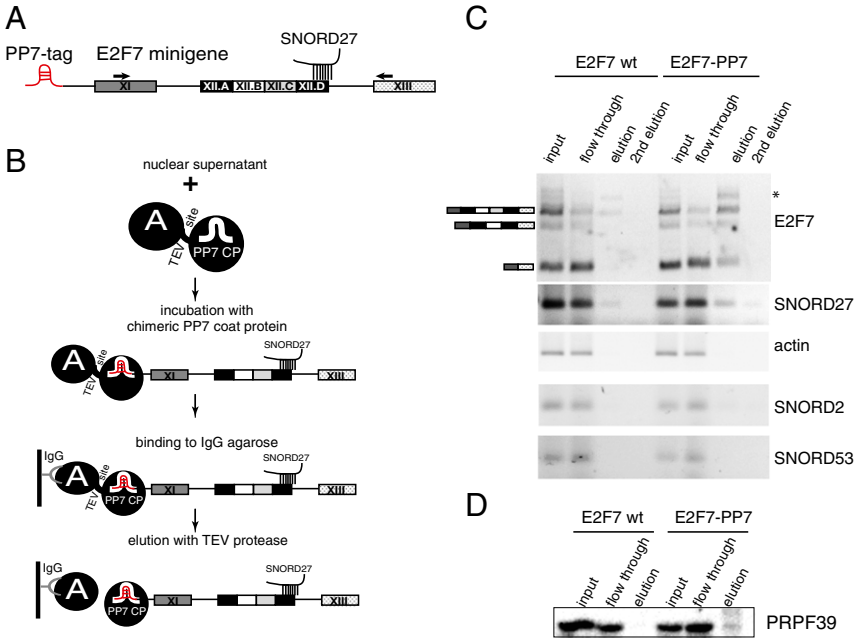


**Fig. 4.** *SNORD27* binds to *E2F7* pre-mRNA in vivo. (*A*) Schematic representation of the E2F7-PP7 minigene with a PP7 RNA tag at the 5′ end. The location of the *SNORD27* binding site and amplification primers are indicated. (*B*) Purification scheme. Soluble nuclear fractions were obtained from *HeLa* cells transfected with PP7-tagged *E2F7* minigene and incubated with PP7 binding protein fused to protein A. Complexes were isolated using IgG-coated beads and eluted using TEV-protease cleavage. The diagram does not depict the spliceosomal complex within which the eluted transcript is associated. (*C*) RT-PCR of RNAs eluted after PP7 tag purification. *E2F7* and *SNORD27* were amplified by RT-PCR, and *SNORD53* and β-actin were used as negative controls. *Location of an unspecific extra band. (*D*) Western blot showing the elution profile of the spliceosome-associated protein *PRPF39*. Lanes correspond to those in *C*.

*E2F7* (Fig. 3*A*). Transfecting the WT *SNORD27* had no statistically significant effect on the splicing pattern of the E2F7 minigene carrying these two nucleotide mutations (Fig. 3*A*). In contrast, using an *SNORD27* compensatory mutation strongly induced exon skipping (Fig. 3*B*). Additional mutations led to almost full alternative exon inclusion (Fig. S5*A*), and cotransfection of *SNORD27* carrying the compensatory mutations did not change the splicing pattern (Fig. S5*C*). These data show that *SNORD27*–target RNA binding is necessary for regulation, indicating a direct binding in vivo.

We next tested whether the *E2F7* alternative exon could be regulated by a heterologous SNORD. We tested *SNORD115*, which has been shown to regulate alternative splicing of the *serotonin receptor 2C* pre-mRNA. We introduced pre-mRNA *serotonin receptor 2C* sequences into the *E2F7* minigene and the *SNORD115* antisense sequence into *SNORD27*. Introducing the serotonin receptor sequences into the *E2F7* exon resulted in its skipping, and *SNORD27* overexpression resulted in a slight activation of the exon (Fig. 3*C*). However, introducing the 18-nt sequence complementarity between *serotonin receptor 2C* pre-mRNA and *SNORD115* into the *E2F7* alternative exon activated the skipping of this exon (Fig. 3*D*), similar to cotransfecting the mutated *E2F7* exon with *SNORD27* containing *SNORD115* sequences (Fig. 3*E*). These responses to compensatory mutations suggest that RNA binding sites can be swapped between pre-mRNA and their regulating SNORDs. However, the exact outcome of the regulation is influenced by the sequence context.

**SNORD27 Associates with E2F7 mRNA in the Nucleus.** The compensatory mutations strongly suggest a direct interaction between *SNORD27* and *E2F7* pre-mRNA that could regulate splicing. We further tested an association between *SNORD27*, *E2F7*, and splicing factors using biochemical pulldown experiments. To allow for RNA pull-down, we introduced the binding site for *Pseudomonas aeruginosa* phage 7 (PP7) coat protein at 5′ end of E2F7 minigene (PP7-tag) (40, 54) (Fig. 4*A*). This system was previously used for affinity purification of native RNP complexes (54). The PP7-tagged construct was transfected into *HeLa* cells, and a soluble native nuclear fraction was prepared (Fig. 1*A*). The supernatant was incubated with a PP7 binding protein fused to two *Z* domains of protein A by a Tobacco etch virus protease (TEV) cleavage site (54), and RNA and associated factors were captured using IgG-agarose beads. *E2F7* RNA and associated factors were released using the TEV protease under native conditions (Fig. 4*B*).

After eluting bound RNA with TEV protease, we could readily detect *E2F7* mRNA as well as *SNORD27* in the eluates, whereas an *E2F7* minigene without PP7 tag produced no signal in the eluates (Fig. 4*C*). An extra faint band, detected above the RT-PCR product of unspliced *E2F7* RNA, likely represents a precursor that has high unspecific binding to the beads, because it was detected in eluates of both untagged control and PP7-tagged E2F7.

Next, we analyzed the same eluates using Western blot with an antibody against the *U1* component PRPF39, which again gave a specific signal in the PP7-E2F7 minigene eluates (Fig. 4*D*). These findings indicate that *SNORD27* binds to *E2F7* RNA during the splicing reaction.

**E2F7 mRNA Is Not 2′-*O*-Methylated in the SNORD27 Binding Site.** Although we could not detect fibrillarin in the soluble nuclear supernatants, the direct interaction between *SNORD27* and *E2F7* could indicate E2F7 2′-*O*-methylation by using catalytic amounts of fibrillarin, which could impact splicing. We tested this possibility using primer extension analysis under limited nucleotide concentration. In this assay, RNA is reverse transcribed with a decreasing concentration of deoxynucleotides, resulting in a pause at the methylation site under limiting conditions (Fig. 5 *A* and *B*). We used this assay to determine the methylation status at A27 of *18S* rRNA and observed a clear pause at the predicted site at 4 μM

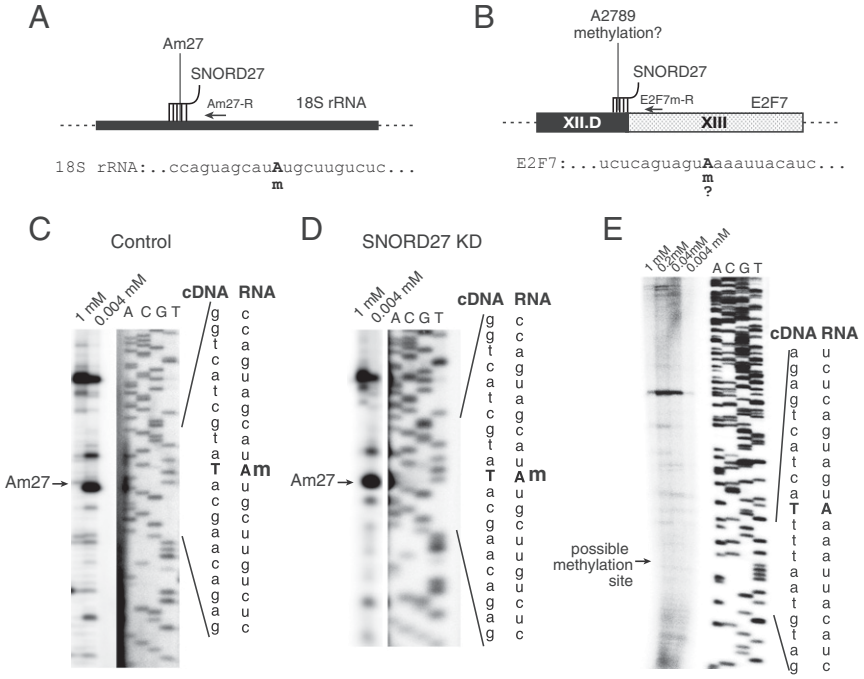


**Fig. 5.** *SNORD27* does not cause 2′-*O*-methylation of E2F7-RNA. The complementarity between *SNORD27* and its targets is indicated in Fig. 2*A*. (*A*) Location of the reverse primer Am27-R and *SNORD27* binding site in the *18S* rRNA. The nucleotide A27 predicted to undergo 2′-*O*-methylation is indicated with an m. (*B*) Location of the reverse primer E2F7m-R and a predicted 2′-*O*-methylation site in the *E2F7* RNA. The nucleotide A2789 (RefSeq NM_2033942) predicted to undergo 2′-*O*-methylation is indicated with an m. (*C*) Primer extension using *18S* rRNA with excess or limited amount of dNTPs using primer Am27-R. (*D*) Primer extension using *18S* rRNA derived from cells treated with *SNORD27* knockdown oligonucleotide. (*E*) Primer extension using *E2F7* RNA with excess or limited amount of dNTPs using primer E2F7m-R. The gels show the cDNA sequence corresponding to the RNA sequence shown on the right. KD, knockdown.

dNTP concentration (Fig. 5*C*). In contrast, there is no stop at the *E2F7* sequence located 5 nt upstream of the D box (Fig. 5*E*). *SNORD27* knockdown did not change the methylation pattern of *18S* RNA, indicating that the splicing changes that we observed are not caused by a deregulation of rRNA (Fig. 5*D*). Although in some instances, this method fails to detect a 2′-*O*-methylation (55), the absence of a reverse transcription stop together with fibrillarin not being detected in nuclear supernatant strongly suggest that *E2F7* pre-mRNA is not methylated.

**SNORD27 Suppresses Silent Exon Inclusion in Multiple Pre-mRNAs.** We next tested more computationally predicted interactions between *SNORD27* and pre-mRNAs (Table S2) by comparing splicing patterns between naive *HeLa* cells and cells undergoing *SNORD27* knockdown.

From 30 *SNORD27* predicted binding sites near alternative exons, eight exons showed alternative splicing in *HeLa* cells. In these events, we observed changes in the splicing patterns for *FER*, *ZBTB37*, *MAP4K3*, and *ABCA8* (Fig. 6) after *SNORD27* knockdown. *SNORD27* knockdown resulted in several unexpected bands. Sequencing revealed the existence of nonannotated exons (Fig. 6 and Table S3*C*), for which no EST evidence was available. Thus, one of the functions of *SNORD27* seems to be to repress the inclusion of putative exons. These putative silent exons have canonical 5′ and 3′ splice sites but were not previously detected in mRNAs.

## Discussion

SNORDs are highly abundant and among the best-studied ncRNAs. In the classic model, the snoRNA forms a complex with NOP58, NOP56, NHP2L1, and the 2′-*O*-methyltransferase fibrillarin. The RNA guides this enzymatic activity predominantly to rRNAs using one or two accessible snoRNA parts, the antisense boxes. However, about one-half of 267 human snoRNAs show no sequence complementarity toward other ncRNAs and thus, are orphan, suggesting additional functions (25, 56). Genome-wide analysis of SNORD–rRNA interaction revealed additional base-pairing regions and suggested an asymmetric binding of proteins to human SNORDs (57). These results indicate that there are differences between SNORDs from different organisms and between individual SNORDs. In addition, orphan SNORDs have shown functions in alternative splicing, cholesterol traffic, microRNAs production, and lipid toxicity (reviewed in ref. 58), but their mechanism of action remained unclear.

To obtain mechanistic insight into these noncanonical functions of SNORDs, we isolated nucleoplasmic SNORDs under native conditions and fractionated them using glycerol gradients.

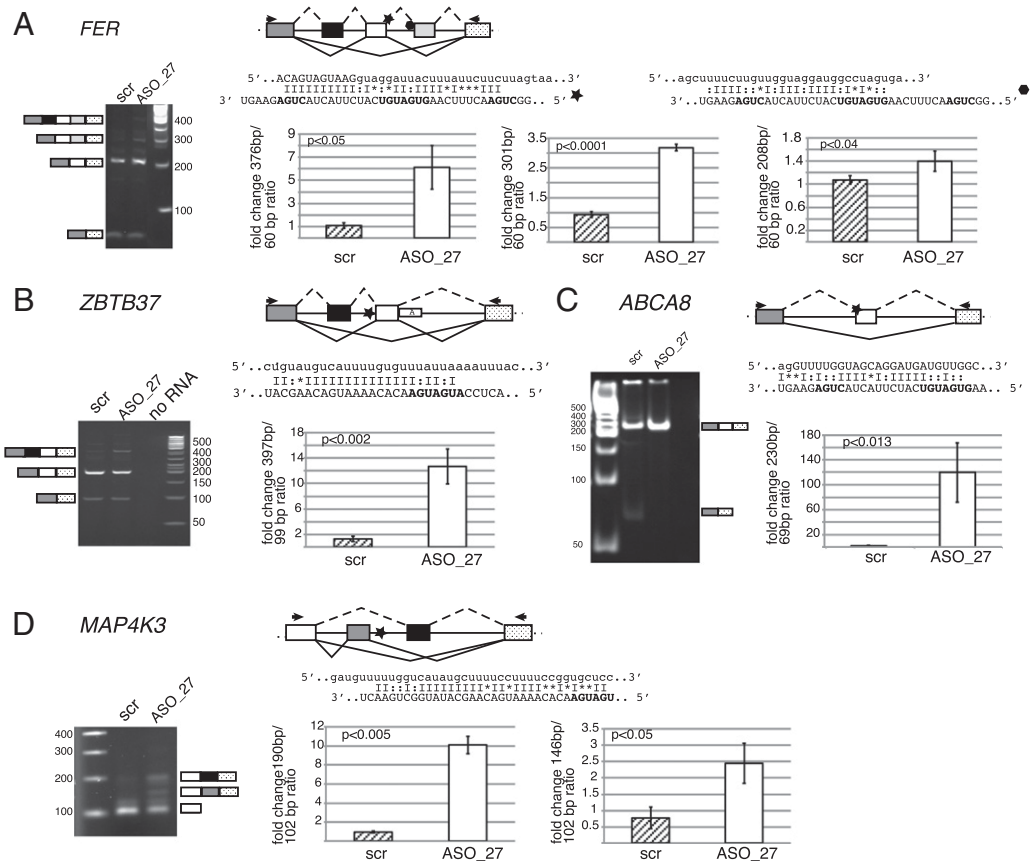


**Fig. 6.** *SNORD27* regulates multiple exons. Validation of bioinformatically predicted *SNORD27* binding sites (Table S2). *HeLa* cells were transfected with *SNORD27* antisense (ASO_27) or random base oligonucleotide (scr), and RNA was analyzed by RT-PCR. The fragments of each investigated gene are shown schematically. Rectangles and lines represent exons and introns, respectively. Black boxes represent silent exons, white and light gray boxes represent alternative exons, and dark gray and dotted boxes constitutive exons. The stars and hexagons show the locations of the *SNORD27* binding sites. Solid lines indicate the splicing patterns observed in *HeLa* cells, and dashed lines indicate the splicing patterns in *HeLa* cells with *SNORD27* knockdown. Sequence alignments show complementarities between *SNORD27* and regulated pre-mRNAs. *SNORD27* is shown in the 3′→5′ direction; all other RNAs are in the 5′→3′ direction. The C and D boxes are indicated in bold. Canonical base pairing is indicated with a line, G:U base pairing is indicated with a dot, and mismatches are indicated with stars. The graphs in *Right* show the quantification of the splicing products. The diagram above each graph shows which ratio was determined. The ratio of exon inclusion to exon skipping of untreated cells was set to one. The fold change is shown. Error bars are SDs of three independent experiments. The *P* values were determined using two-tailed *t* tests. Effect of *SNORD27* knockdown on alternative splicing of the following gene transcripts: (*A*) *FER*, (*B*) *ZBTB37*, (*C*) *ABCA8*, and (*D*) *MAP4K3*.

RNA-seq of fractions that contained the pre-mRNA splicing machinery but were devoid of fibrillarin showed that a subset of SNORDs is present in these fractions, including SNORDs known to target rRNA. Because the canonical SNORD protein fibrillarin was not detectable, these SNORDs do not form canonical RNPs and do not function in RNA methylation. Not all SNORDs expressed in *HeLa* cells are present in these native fractions, and some SNORDs seems to be enriched (Fig. S1*B* and Table S1), which argues against a dissociation of snoRNPs during the isolation procedure that would affect all SNORDs. SNORDs were more abundant in this preparation than H/ACA box snoRNAs. This enrichment may reflect the biogenesis of SNORDs, in that they are released by exonucleases acting on introns released by the spliceosome. In contrast, the generation of H/ACA box snoRNAs is less dependent on splicing (59). Thus, it is possible that, because of their biogenesis, some SNORDs can be retained by the spliceosome, where they could play a role in splice site selection. It is also possible that retention occurs through the NHP2L1 protein, which is a component of both the SNORDs and the *U4*/*U6* complex—a hypothesis that needs to be investigated in the future.

We focused on *SNORD27* as an example, because it is deregulated during the progression of smoldering multiple myeloma (21). *SNORD27* is not an orphan SNORD, because it exhibits a perfect sequence complementarity to *18S* RNA and is predicted to methylate A27 (60), which is methylated in human rRNA. Computational searches revealed a 29-nt-long stretch of complementarity between *SNORD27* and the pre-mRNA of the *E2F7* transcription factor. This complementarity contains two G:U base pairing and four mismatched bases. Importantly, the C′ and D′ boxes of *SNORD27* are part of the sequence complementarity. Their inclusion in the binding site further suggests the noncanonical nature of this *SNORD27* complex; as in a canonical snoRNP, these sequences bind to their respective C and D boxes and interact with proteins (6). Furthermore, the involvement of C and D boxes in pre-mRNA binding might explain why we could not detect 2′-*O*-methylation of *E2F7* pre-mRNA.

On the pre-mRNA level, the sequence complementarity encompasses seven of nine bases at the 5′ splice site that bind to U1 snRNA during the splicing reaction. Overexpression of *SNORD27* leads to skipping of the exon and knockdown of *SNORD27* results in increased exon inclusion, suggesting that *SNORD27* inhibits alternative exon use. The analysis of compensatory mutations and RNA pulldown experiments suggests that *SNORD27* binds directly to *E2F7* pre-mRNAs. The location of the binding site near the 5′ splice site suggests that *SNORD27* acts through competition with *U1* snRNP. The correct regulation of the *E2F7* alternative exon is likely important for the cell, because use of the exon changes the reading frame and alters the C terminus of the protein, which is necessary for the transcriptional activation of its target genes. *E2F7* has antiproliferative properties (61, 62), and it is possible that *SNORD27* changes observed in cancer influence E2F7-dependent cell cycle regulation.

*SNORD27* binding sites in 30 human genes were predicted computationally (Table S2). From this list, *SNORD27* knockdown identified four genes with alternative splicing that is influenced by *SNORD27* in *HeLa* cells. In one of the identified genes, *FER*, the sequence complementarity between *SNORD27* and the pre-mRNA encompasses the 5′ splice, and therefore, the *SNORD27* could act through competition with *U1* snRNP. The binding site in the *ABCA8* pre-mRNA covers a 3′ splice site, possibly affecting *U2AF* binding. The other sequence complementarities are in intronic regions, and the mechanism of action is unclear. Detailed mechanism of this regulation remains to be determined, but these results indicate that the mechanistic mode of action may differ depending on the binding site of the snoRNA on the pre-mRNA.

The exons regulated by *SNORD27* in the *E2F7*, *FER*, *ZBTB37*, *MAP4K3*, and *ABCA8* genes are all suboptimal. For example, the *E2F7* exon is 425 nt in length, which is abnormally long for a cassette exon. The *SNORD27*-dependent exons in the other genes are flanked by weak splice sites, and there is no EST evidence for their existence in cells. Using RT-PCR, these exons could not be detected without *SNORD27* knockdown. A biological function of *SNORD27* could thus be the repression of pre-mRNA sequences that have the potential to be recognized as weak alternative exons. Because some of these weak exons are generated through short (Alu) or long (LINE) interspersed elements (63–65), SNORDs might have a more general role in suppressing newly formed exons.

Mechanistically, this regulation of alternative splicing is likely achieved by the formation of a protein–*SNORD27* complex, likely including heterogeneous ribonucleoprotein (hnRNP) proteins, that binds to pre-mRNAs. *SNORD27* is equally distributed throughout a 10–45% glycerol gradient (Fig. 1*D*), suggesting that it forms protein complexes of differing composition. In contrast, *SNORD2* and *SNORD60* peak at low glycerol concentrations, suggesting a unique SNORD–protein complex (Fig. S3). To gain insight into proteins associated with *SNORD27*, we pulled down *SNORD27* from soluble nuclear fractions using RNA capture oligos and identified associated proteins using MS (Fig. S6). These proteins were predominantly RNA binding proteins, including hnRNPs, which might associate with *SNORD27*. However, the precise nature of these hnRNP–*SNORD27* complexes remains to be determined.

The sequence complementarities between *SNORD27* and all of its targets contained the C and D boxes of *SNORD27* (Fig. 7*A*). The presence of C and D boxes in the binding sites indicates that the whole SNORD sequence has to be analyzed to identify target genes. As with other SNORDs, the RPA of *SNORD27* showed the occurrence of smaller fragments (Fig. 1*D*). It is currently unclear whether the shorter fragments or the full-length

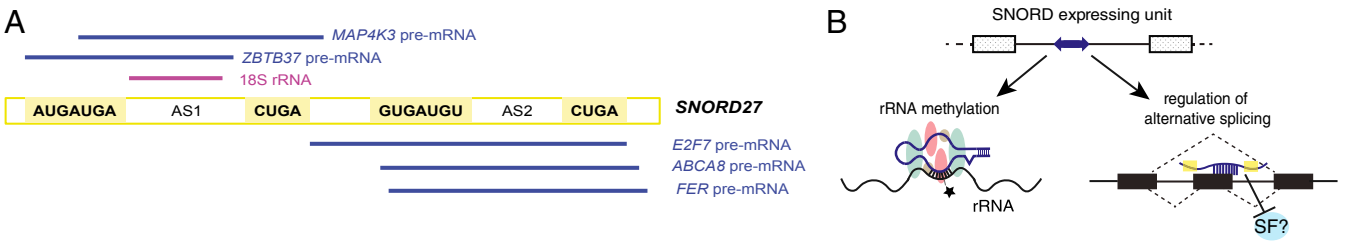


**Fig. 7.** A dual role for *SNORD27* in rRNA and pre-mRNA processing. (*A*) Regions of complementarity between *SNORD27* and its pre-mRNA and rRNA targets. The C (RUGAUGA), D (CUGA), and antisense boxes (AS1 and AS2) are indicated. Lines indicate the sequence complementarity toward regulated pre-mRNAs and *18S* rRNA. The detailed RNA sequences are shown in Figs. 2*A* and 6. (*B*) Working model for *SNORD27* action on pre-mRNA regulation. (*B*, *Lower Left*) *SNORD27* can associate with NOP56, NOP58, NHP2L1, and fibrillarin to form a canonical snoRNP that performs 2′-*O*-methylation on rRNA (*B*, *Lower Right*). A portion of the snoRNA associates with RNA binding proteins and regulates pre-mRNA splicing, where it represses exons, possibly by competing with activating splicing factors, such as *U1* snRNA, or other splicing factors (SFs).

snoRNA is active in splice site regulation. Because the full-length snoRNA is more abundant for *SNORD27*, we assume that the full-length form is the active one.

An evolutionary analysis (Table S3*D*) shows that the first antisense box binding to *18S* rRNA is highly conserved between *SNORD27* orthologs. However, sequences corresponding to the *E2F7* interaction site are highly divergent during evolution without compensatory mutations in the *E2F7* genes (Table S3*E*). Thus, searches for noncanonical SNORD targets should not take evolutionary conservation into account and should include the whole sequence, not just the antisense boxes. Furthermore, *SNORD27* fragments have also been observed in mouse retinas, where 19-, 26-, and 28-nt-long fragments were identified by deep sequencing (66), suggesting a conservation of noncanonical properties. It is possible that SNORD regulation of alternative splicing is species-specific, possibly reflecting the low conservation of alternative frameshifting exons between species (67, 68). In this scenario, newly evolved alternative exon use could be regulated by interaction with SNORDs.

Several SNORDs and H/ACA box snoRNAs have been shown to be precursors for microRNAs (69, 70). Consistent with our observations, Brameier et al. (70) found that *SNORD27* [designated as *U27* sno-miRNA (for snoRNA derived microRNA)] generates short stable fragments of ∼20 nt in length. However, the physiological function of these fragments remains unclear, because *U27* sno-miRNA did not cause an effect in a Renilla/Luciferase reporter system in *HeLa* cells.

Our finding that numerous SNORDs predicted to modify rRNA, among them *SNORD27*, *SNORD2*, *SNORD60*, and *SNORD78*, can be detected in fractions where fibrillarin was not detected suggests that canonical SNORDs have biological roles in addition to their involvement in 2′-*O*-methylation. Importantly, assays that solely rely on detecting the association with fibrillarin (71) will miss these previously unidentified, noncanonical functions, because they do not take localization in a fibrillarin-free fraction into account. It is possible that the unexpected role of *SNORD60* in intracellular cholesterol trafficking is caused through a fibrillarin-free RNP acting on pre-mRNAs and not through rRNA methylation (19).

As exemplified by *SNORD27*, an SNORD can function in both pre-mRNA and rRNA metabolism (Fig. 7*B*). Findings in yeast suggest that cells can regulate the assembly of snoRNAs into SNORD-RNPs through the R2TP complex (26, 27). It is thus possible that a cell can regulate the fraction of SNORDs acting in pre-mRNA or rRNA processing. For example, cells might use more *SNORD27* for rRNA modification when there is demand for protein biosynthesis. This model suggests that SNORDs could participate in coordinating mRNA processing with ribosomal biogenesis.

More than 2,500 transcription factors have been identified in humans (72). In contrast, less than 50 sequence-specific splicing regulators have been described (73). It is possible that ncRNAs provide additional sequence-specific splicing regulation, and we suggest that this is a novel role for some SNORDs.

## Materials and Methods

**Preparation of Soluble Nuclear Supernatant Under Native Conditions.** Nuclear supernatant was prepared as previously described with minor modifications (36, 37). *HeLa* cells, grown in five 15-cm Petri dishes, were washed two times in VB buffer [0.125 M KCl, 30 mM Tris·HCl, pH 7.5, 5 mM $Mg(oAc)_2$, 0.15 mM spermine, 0.05 mM spermidine, 2 mM vanadyl ribonucleosides], resuspended in isotonic SB buffer [10 mM KCl, 30 mM Tris·HCl, pH 7.5, 5 mM $Mg(OAc)_2$, 0.15 mM spermine, 0.05 mM spermidine, 2 mM vanadyl ribonucleosides], and opened with 20 strokes in Dounce homogenizer (pestle B). Cell nuclei were layered on the glycerol cushion [25% (vol/vol) glycerol, 10 mM KCl, 30 mM Tris·HCl, pH 7.5, 5 mM $Mg(oAc)_2$, 0.15 mM spermine, 0.05 mM spermidine, 2 mM vanadyl ribonucleosides]. After centrifugation for 4 min at 4,000 × *g*, the aqueous layer was designated as "cytoplasm," and the pellet was designated as "crude nuclei." Nuclei pellet was washed two times, resuspended in ST2M buffer (0.1 M NaCl, 10 mM Tris·HCl, pH 8.0, 2 mM $MgCl_2$, 0.15 mM spermine, 0.05 mM spermidine, 2 mM vanadyl ribonucleosides), and sonicated using a Bioraptor Plus (Diagenode) instrument (two cycles of 30-s pulse and 30-s break; setting: high). After chromatin precipitation in the presence of 2 mg/mL yeast tRNA (Life Technology), sample was cleared by centrifugation (3 min at 13,500 × *g*), and resulting supernatant was designated as "nuclear supernatant." The pellet was resuspended in 1× RIPA buffer (0.15 M NaCl, 50 mM Tris·HCl, pH 8.0, 1% Nonidet P-40, 0.5% sodium deoxycholate, protease inhibitor mixture), sonicated using a Bioraptor instrument (three cycles of 30-s pulse and 30-s break; setting: high), and cleared. The supernatant was designated as "resuspended nuclear pellet."

**RNA Isolation and RNA-Seq.** Nuclear supernatant (described above) was fractionated using 10–45% (vol/vol) glycerol gradients (37). Centrifugations were carried out at 4 °C in an SW41 rotor run at 41,000 rpm (287,472 × *g*) for 90 min. Fractions cosedimenting with splicing factors (8–11; sedimenting at 200S) were pooled, and RNA was isolated and analyzed. To extract RNA associated with the spliceosomes, fractions of the glycerol gradients (520 μL) were mixed with 150 μL extraction buffer (50 mM Tris·HCl, pH 7.5, 300 mM NaCl) and 50 μL 10% (wt/vol) SDS, and the RNA was recovered by extraction with phenol and precipitation in ethanol (37). The integrity of the RNA was evaluated by an Agilent 2100 BioAnalyzer. For small RNA library construction, ∼10 μg RNA was used followed by Illumina Directional mRNA-Seq Library Prep. The prerelease protocol was used with the following changes: (*i*) the poly-A selection and fragmentation of mRNA steps were omitted; and (*ii*) to enrich for small RNAs, ethanol precipitation was used instead of column fractionation of the T4 polynucleotide kinase-treated RNA. Adaptors were then ligated to the 5′ and 3′ ends of the RNA, and cDNA was prepared from the ligated RNA and amplified to prepare the sequencing library. The amplified sequences were purified by PAGE, and sequences representing RNA smaller than 200 nt were extracted from the gel. The library was sequenced using the Genome AnalyzerIIX System by Illumina.

*SI Materials and Methods* describes cell lines, analysis of sequencing data, PP7-tagged RNA affinity purification, immunoprecipitation and RNA isolation, methylation analysis, protein analysis by Western blot, purification of the recombinant proteins, RNase protection analysis, list of primers, RT-PCR, purification of RNA and bound proteins using biotinylated antisense oligonucleotides, and MS and protein identifications.

**ACKNOWLEDGMENTS.** The authors thank N. J. McGlincy, C. Waechter, K. Collins, and G. Grohs for discussions. We thank the University of Kentucky Proteomics Core, which was supported by National Institute of General Medical Sciences Centers of Biomedical Research Excellence Grant P20GM103486-09 and the Office of the Vice President for Research of the University of Kentucky as well as High-End Instrumentation Grant S10RR029127. This work was supported by Postdoctoral Fellowship 13POST16820024 from the American Heart Association (to M.F.); MINECO (Ministerio de Economía y Competitividad) Spanish Government Grant BIO2014-52566-R (to A.P. and E.E.); Consolider RNAREG Grant CSD2009-00080 (to A.P. and E.E.); Sandra Ibarra Foundation for Cancer Grant FSI2013 (to A.P. and E.E.); AGAUR (Agència de Gestió d'Ajuts Universitaris i de Recerca) Grant 2014-SGR1121 (to A.P. and E.E.); USA-Israel Binational Science Foundation, Transformative Grant 2010508 (to R.S. and S.S.); NIH Grants 01GM079549 (to R.S.) and 01GM083187 (to S.S.); and the Foundation for Prader-Willi Research (S.S.).

1. Filipowicz W, Pelczar P, Pogacic V, Dragon F (1999) Structure and biogenesis of small nucleolar RNAs acting as guides for ribosomal RNA modification. *Acta Biochim Pol* 46(2):377–389.
2. Filipowicz W, Pogacić V (2002) Biogenesis of small nucleolar ribonucleoproteins. *Curr Opin Cell Biol* 14(3):319–327.
3. Watkins NJ, Bohnsack MT (2012) The box C/D and H/ACA snoRNPs: Key players in the modification, processing and the dynamic folding of ribosomal RNA. *Wiley Interdiscip Rev RNA* 3(3):397–414.
4. Hirose T, Shu MD, Steitz JA (2003) Splicing-dependent and -independent modes of assembly for intron-encoded box C/D snoRNPs in mammalian cells. *Mol Cell* 12(1):113–123.
5. Bizarro J, et al. (2014) Proteomic and 3D structure analyses highlight the C/D box snoRNP assembly mechanism and its control. *J Cell Biol* 207(4):463–480.
6. Lapinaite A, et al. (2013) The structure of the box C/D enzyme reveals regulation of RNA methylation. *Nature* 502(7472):519–523.
7. Hüttenhofer A, et al. (2001) RNomics: An experimental approach that identifies 201 candidates for novel, small, non-messenger RNAs in mouse. *EMBO J* 20(11):2943–2953.
8. Jády BE, Kiss T (2000) Characterisation of the U83 and U84 small nucleolar RNAs: Two novel 2′-O-ribose methylation guide RNAs that lack complementarities to ribosomal RNAs. *Nucleic Acids Res* 28(6):1348–1354.
9. Cavaillé J, et al. (2000) Identification of brain-specific and imprinted small nucleolar RNA genes exhibiting an unusual genomic organization. *Proc Natl Acad Sci USA* 97(26):14311–14316.
10. Vitali P, et al. (2003) Identification of 13 novel human modification guide RNAs. *Nucleic Acids Res* 31(22):6543–6551.

11. Saraiya AA, Wang CC (2008) snoRNA, a novel precursor of microRNA in Giardia lamblia. *PLoS Pathog* 4(11):e1000224.
12. Hutzinger R, et al. (2009) Expression and processing of a small nucleolar RNA from the Epstein-Barr virus genome. *PLoS Pathog* 5(8):e1000547.
13. Taft RJ, et al. (2009) Small RNAs derived from snoRNAs. *RNA* 15(7):1233–1240.
14. Kawaji H, et al. (2008) Hidden layers of human small RNAs. *BMC Genomics* 9: 157.
15. Scott MS, Avolio F, Ono M, Lamond AI, Barton GJ (2009) Human miRNA precursors with box H/ACA snoRNA features. *PLOS Comput Biol* 5(9):e1000507.
16. Ono M, et al. (2011) Identification of human miRNA precursors that resemble box C/D snoRNAs. *Nucleic Acids Res* 39(9):3879–3891.
17. Ding F, et al. (2008) SnoRNA Snord116 (Pwcr1/MBII-85) deletion causes growth deficiency and hyperphagia in mice. *PLoS One* 3(3):e1709.
18. Duker AL, et al. (2010) Paternally inherited microdeletion at 15q11.2 confirms a significant role for the SNORD116 C/D box snoRNA cluster in Prader-Willi syndrome. *Eur J Hum Genet* 18(11):1196–1201.
19. Brandis KA, et al. (2013) Box C/D small nucleolar RNA (snoRNA) U60 regulates intracellular cholesterol trafficking. *J Biol Chem* 288(50):35703–35713.
20. Michel CI, et al. (2011) Small nucleolar RNAs U32a, U33, and U35a are critical mediators of metabolic stress. *Cell Metab* 14(1):33–44.
21. López-Corral L, et al. (2012) Genomic analysis of high-risk smoldering multiple myeloma. *Haematologica* 97(9):1439–1443.
22. Dong XY, et al. (2009) Implication of snoRNA U50 in human breast cancer. *J Genet Genomics* 36(8):447–454.
23. Dong XY, et al. (2008) SnoRNA U50 is a candidate tumor-suppressor gene at 6q14.3 with a mutation associated with clinically significant prostate cancer. *Hum Mol Genet* 17(7):1031–1042.
24. Siprashvili Z, et al. (2016) The noncoding RNAs SNORD50A and SNORD50B bind K-Ras and are recurrently deleted in human cancer. *Nat Genet* 48(1):53–58.
25. Deschamps-Francoeur G, et al. (2014) Identification of discrete classes of small nucleolar RNA featuring different ends and RNA binding protein dependency. *Nucleic Acids Res* 42(15):10073–10085.
26. Kakihara Y, Makhnevych T, Zhao L, Tang W, Houry WA (2014) Nutritional status modulates box C/D snoRNP biogenesis by regulated subcellular relocalization of the R2TP complex. *Genome Biol* 15(7):404.
27. Prieto MB, Georg RC, Gonzales-Zubiate FA, Luz JS, Oliveira CC (2015) Nop17 is a key R2TP factor for the assembly and maturation of box C/D snoRNP complex. *BMC Mol Biol* 16:7.
28. Pan Q, et al. (2005) Alternative splicing of conserved exons is frequently species-specific in human and mouse. *Trends Genet* 21(2):73–77.
29. Wang ET, et al. (2008) Alternative isoform regulation in human tissue transcriptomes. *Nature* 456(7221):470–476.
30. Kelemen O, et al. (2013) Function of alternative splicing. *Gene* 514(1):1–30.
31. Kishore S, Stamm S (2006) The snoRNA HBII-52 regulates alternative splicing of the serotonin receptor 2C. *Science* 311(5758):230–232.
32. Scott MS, et al. (2012) Human box C/D snoRNA processing conservation across multiple cell types. *Nucleic Acids Res* 40(8):3676–3688.
33. Zhao X, Yu YT (2008) Targeted pre-mRNA modification for gene silencing and regulation. *Nat Methods* 5(1):95–100.
34. Ge J, Liu H, Yu YT (2010) Regulation of pre-mRNA splicing in Xenopus oocytes by targeted 2′-O-methylation. *RNA* 16(5):1078–1085.
35. Stepanov GA, et al. (2013) Artificial box C/D RNAs affect pre-mRNA maturation in human cells. *BioMed Res Int* 2013:656158.
36. Spann P, Feinerman M, Sperling J, Sperling R (1989) Isolation and visualization of large compact ribonucleoprotein particles of specific nuclear RNAs. *Proc Natl Acad Sci USA* 86(2):466–470.
37. Azubel M, Habib N, Sperling R, Sperling J (2006) Native spliceosomes assemble with pre-mRNA to form supraspliceosomes. *J Mol Biol* 356(4):955–966.
38. Dignam JD, Lebovitz RM, Roeder RG (1983) Accurate transcription initiation by RNA polymerase II in a soluble extract from isolated mammalian nuclei. *Nucleic Acids Res* 11(5):1475–1489.
39. Sperling R, Spann P, Offen D, Sperling J (1986) U1, U2, and U6 small nuclear ribonucleoproteins (snRNPs) are associated with large nuclear RNP particles containing transcripts of an amplified gene in vivo. *Proc Natl Acad Sci USA* 83(18):6721–6725.
40. Kotzer-Nevo H, de Lima Alves F, Rappsilber J, Sperling J, Sperling R (2014) Supraspliceosomes at defined functional states portray the pre-assembled nature of the pre-mRNA processing machine in the cell nucleus. *Int J Mol Sci* 15(7):11637–11664.
41. Yitzhaki S, Miriami E, Sperling R, Sperling J (1996) Phosphorylated Ser/Arg-rich proteins: Limiting factors in the assembly of 200S large nuclear ribonucleoprotein particles. *Proc Natl Acad Sci USA* 93(17):8830–8835.
42. Sperling R, et al. (1985) Abundant nuclear ribonucleoprotein form of CAD RNA. *Mol Cell Biol* 5(3):569–575.
43. Sebbag-Sznajder N, et al. (2012) Regulation of alternative splicing within the supraspliceosome. *J Struct Biol* 177(1):152–159.
44. Heinrich B, et al. (2009) Heterogeneous nuclear ribonucleoprotein G regulates splice site selection by binding to CC(A/C)-rich regions in pre-mRNA. *J Biol Chem* 284(21): 14303–14315.
45. Yang YH, et al. (2013) ZRANB2 localizes to supraspliceosomes and influences the alternative splicing of multiple genes in the transcriptome. *Mol Biol Rep* 40(9): 5381–5395.
46. Lestrade L, Weber MJ (2006) snoRNA-LBME-db, a comprehensive database of human H/ACA and C/D box snoRNAs. *Nucleic Acids Res* 34(Database issue):D158–D162.
47. Consortium EP; ENCODE Project Consortium (2012) An integrated encyclopedia of DNA elements in the human genome. *Nature* 489(7414):57–74.
48. Sperling J, Azubel M, Sperling R (2008) Structure and function of the Pre-mRNA splicing machine. *Structure* 16(11):1605–1615.
49. Shefer K, Sperling J, Sperling R (2014) The supraspliceosome—a multi-task machine for regulated pre-mRNA processing in the cell nucleus. *Comput Struct Biotechnol J* 11(19):113–122.
50. Raitskin O, Cho DS, Sperling J, Nishikura K, Sperling R (2001) RNA editing activity is associated with splicing factors in lnRNP particles: The nuclear pre-mRNA processing machinery. *Proc Natl Acad Sci USA* 98(12):6571–6576.
51. Kishore S, et al. (2010) The snoRNA MBII-52 (SNORD 115) is processed into smaller RNAs and regulates alternative splicing. *Hum Mol Genet* 19(7):1153–1164.
52. Bolisetty MT, Beemon KL (2012) Splicing of internal large exons is defined by novel cis-acting sequence elements. *Nucleic Acids Res* 40(18):9244–9254.
53. Ideue T, Hino K, Kitao S, Yokoi T, Hirose T (2009) Efficient oligonucleotide-mediated degradation of nuclear noncoding RNAs in mammalian cultured cells. *RNA* 15(8): 1578–1587.
54. Hogg JR, Collins K (2007) RNA-based affinity purification reveals 7SK RNPs with distinct composition and regulation. *RNA* 13(6):868–880.
55. Maden BE (2001) Mapping 2′-O-methyl groups in ribosomal RNA. *Methods* 25(3): 374–382.
56. Dupuis-Sandoval F, Poirier M, Scott MS (2015) The emerging landscape of small nucleolar RNAs in cell biology. *Wiley Interdiscip Rev RNA* 6(4):381–397.
57. van Nues RW, et al. (2011) Box C/D snoRNP catalysed methylation is aided by additional pre-rRNA base-pairing. *EMBO J* 30(12):2420–2430.
58. Falaleeva M, Stamm S (2012) *Fragments of Small Nucleolar RNAs as a New Source for Non-Coding RNAs. Regulatory RNAs, Basics, Methods and Applications*, eds Mallick B, Ghosh Z (Springer, Berlin), pp 49–71.
59. Richard P, Kiss AM, Darzacq X, Kiss T (2006) Cotranscriptional recognition of human intronic box H/ACA snoRNAs occurs in a splicing-independent manner. *Mol Cell Biol* 26(7):2540–2549.
60. Tycowski KT, Shu MD, Steitz JA (1996) A mammalian gene with introns instead of exons generating stable RNA products. *Nature* 379(6564):464–466.
61. Carvajal LA, Hamard PJ, Tonnessen C, Manfredi JJ (2012) E2F7, a novel target, is up-regulated by p53 and mediates DNA damage-dependent transcriptional repression. *Genes Dev* 26(14):1533–1545.
62. Aksoy O, et al. (2012) The atypical E2F family member E2F7 couples the p53 and RB pathways during cellular senescence. *Genes Dev* 26(14):1546–1557.
63. Lev-Maor G, Sorek R, Shomron N, Ast G (2003) The birth of an alternatively spliced exon: 3′ splice-site selection in Alu exons. *Science* 300(5623):1288–1291.
64. Mersch B, Sela N, Ast G, Suhai S, Hotz-Wagenblatt A (2007) SERpredict: Detection of tissue- or tumor-specific isoforms generated through exonization of transposable elements. *BMC Genet* 8:78.
65. Sela N, Mersch B, Hotz-Wagenblatt A, Ast G (2010) Characteristics of transposable element exonization within human and mouse. *PLoS One* 5(6):e10907.
66. Soundara Pandi SP, Chen M, Guduric-Fuchs J, Xu H, Simpson DA (2013) Extremely complex populations of small RNAs in the mouse retina and RPE/choroid. *Invest Ophthalmol Vis Sci* 54(13):8140–8151.
67. Merkin J, Russell C, Chen P, Burge CB (2012) Evolutionary dynamics of gene and isoform regulation in Mammalian tissues. *Science* 338(6114):1593–1599.
68. Zhang C, Krainer AR, Zhang MQ (2007) Evolutionary impact of limited splicing fidelity in mammalian genes. *Trends Genet* 23(10):484–488.
69. Ender C, et al. (2008) A human snoRNA with microRNA-like functions. *Mol Cell* 32(4): 519–528.
70. Brameier M, Herwig A, Reinhardt R, Walter L, Gruber J (2011) Human box C/D snoRNAs with miRNA like functions: Expanding the range of regulatory RNAs. *Nucleic Acids Res* 39(2):675–686.
71. Bortolin-Cavaillé ML, Cavaillé J (2012) The SNORD115 (H/MBII-52) and SNORD116 (H/MBII-85) gene clusters at the imprinted Prader-Willi locus generate canonical box C/D snoRNAs. *Nucleic Acids Res* 40(14):6800–6807.
72. Babu MM, Luscombe NM, Aravind L, Gerstein M, Teichmann SA (2004) Structure and evolution of transcriptional regulatory networks. *Curr Opin Struct Biol* 14(3):283–291.
73. Chen M, Manley JL (2009) Mechanisms of alternative splicing regulation: Insights from molecular and genomics approaches. *Nat Rev Mol Cell Biol* 10(11):741–754.
74. Kim D, et al. (2013) TopHat2: Accurate alignment of transcriptomes in the presence of insertions, deletions and gene fusions. *Genome Biol* 14(4):R36.
75. Wang WC, et al. (2009) miRExpress: Analyzing high-throughput sequencing data for profiling microRNA expression. *BMC Bioinformatics* 10:328.
76. Rosenbloom KR, et al. (2013) ENCODE data in the UCSC Genome Browser: Year 5 update. *Nucleic Acids Res* 41(Database issue):D56–D63.
77. Quinlan AR, Hall IM (2010) BEDTools: A flexible suite of utilities for comparing genomic features. *Bioinformatics* 26(6):841–842.
78. Kiss T, Jády BE (2004) Functional characterization of 2′-O-methylation and pseudouridylation guide RNAs. *Methods Mol Biol* 265:393–408.
79. Convertini P, et al. (2014) Sudemycin E influences alternative splicing and changes chromatin modifications. *Nucleic Acids Res* 42(8):4947–4961.
80. Kapust RB, et al. (2001) Tobacco etch virus protease: Mechanism of autolysis and rational design of stable mutants with wild-type catalytic proficiency. *Protein Eng* 14(12):993–1000.
81. Trapnell C, Pachter L, Salzberg SL (2009) TopHat: Discovering splice junctions with RNA-Seq. *Bioinformatics* 25(9):1105–1111.
82. Pappin DJ, Hojrup P, Bleasby AJ (1993) Rapid identification of proteins by peptide-mass fingerprinting. *Curr Biol* 3(6):327–332.